Fourier analysis of stabilised Q1-Q1 mixed finite element approximation

Norburn, Sean and Silvester, David J.

2001

MIMS EPrint: **2006.337**

ISSN 1749-9097

SIAM J. NUMER. ANAL.
Vol. 39, No. 3, pp. 817–833

FOURIER ANALYSIS OF STABILIZED Q_1-Q_1 MIXED FINITE ELEMENT APPROXIMATION*

SEAN NORBURN† AND DAVID SILVESTER†

Abstract. We use Fourier analysis to investigate the instability of an equal-order mixed finite element approximation method for elliptic incompressible flow equations. The lack of stability can be attributed to the fact that the associated discrete Ladyzhenskaya–Babuška–Brezzi (LBB) constant tends to zero as the mesh size is reduced. We develop a stabilization approach that is appropriate to the periodic setting and deduce optimal choices of the associated stabilization parameter.

Key words. finite element, mixed approximation, stabilization

AMS subject classifications. 65N15, 65N30

PII. S0036142999362274

1. Introduction.

In recent years, computationally convenient stable low-order discretization methods have been developed for the Stokes and Navier–Stokes equations modelling the steady-state flow of an incompressible fluid. These so-called "stabilized formulations" are widely used by practitioners since they permit the use of equal-order velocity and pressure approximations—a combination that is notoriously unstable in the standard finite element framework. The drawback with this methodology is the introduction of stabilization parameters that must be chosen sensibly if the resulting method is to work well in practice; see Norburn and Silvester [8]. Although the choice of such parameters has been addressed in our previous work (see, e.g., [10], [11]), the characterization of *optimal* parameter choices is not yet resolved. This is the motivation for this work.

For simplicity we restrict our attention to two-dimensional flow problems: the generalization to three-dimensional approximation is quite straightforward. An outline of the paper is as follows. In section 2, the analysis of periodic Stokes flow problems is reviewed. Discretization using a Q_1-Q_1 mixed (C^0 bilinear velocity and pressure) finite element method is then outlined in section 3. In section 4, we analyze the stability of the discrete approximation using standard Fourier analysis techniques. (Although this is a classical approach, the only other work we know of that addresses Ladyzhenskaya–Babuška–Brezzi (LBB) stability from this viewpoint is that of Idelsohn, Storti, and Nigro [7].) Section 5 contains the novel contribution: we consider a standard stabilization technique (originally introduced by Brezzi and Pitkäranta [1] in the case of P_1-P_1 mixed approximation) and deduce the optimal choice of stabilization parameter which minimizes the condition number of the Schur complement matrix that determines stability. Contrary to our expectations, it turns out that the optimal parameter is *not* uniquely determined—there is an interval of parameter values over which optimality is achieved.

2. Periodic Stokes flow formulations.

In order to define a periodic flow problem we need to introduce the concept of periodicity. To this end, let Φ be a vector or scalar field defined over $\mathbb{R}^2$; then Φ is said to be *periodic* in $\mathbf{x}$ (over $\mathbb{R}^2$) with period

*Received by the editors September 27, 1999; accepted for publication (in revised form) February 6, 2001; published electronically June 26, 2001.
http://www.siam.org/journals/sinum/39-3/36227.html

†Department of Mathematics, UMIST, Manchester M60 1QD, UK (na.silvester@na-net.ornl.gov).
The first author's research was supported by EPSRC grant GR/K91262.

$\mathbf{L}$ if

$$\Phi(\mathbf{x}+\mathbf{L}) = \Phi(\mathbf{x}) \quad \forall \mathbf{x} \in \mathbb{R}^2.$$

In general, the vector $\mathbf{L}$ defines a rectangular $L_x \times L_y$ *period cell* $C \subset \mathbb{R}^2$ with boundary $\partial C = \bigcup_{i=1}^4 \partial C_i$ such that

$$\Phi|_{\partial C_1} = \Phi|_{\partial C_3}, \tag{1}$$

$$\Phi|_{\partial C_2} = \Phi|_{\partial C_4}. \tag{2}$$

However, to simplify notation it is convenient to consider flows which have the same periodicity in both coordinate directions; thus we choose the cell $C{=}[0,L] \times [0,L]$.

The regularity of functions defined over C may be classified in terms of their Fourier series expansion. To this end, let $\mathbb{Z}^2{=}\mathbb{Z}{\times}\mathbb{Z}$ and consider

$$\Phi = \sum_{\mathbf{k}\in\mathbb{Z}^2} c_{\mathbf{k}} \exp \frac{2\pi \mathrm{i}\mathbf{k}\cdot\mathbf{x}}{\mathbf{L}}, \qquad \text{where} \quad c_{\mathbf{k}} \in \mathbb{C} \quad \text{with} \quad \bar{c_{\mathbf{k}}} = c_{-\mathbf{k}} \ \forall \mathbf{k} \in \mathbb{Z}^2.$$

The usual scale of Sobolev spaces, $H_p^m(C)$, $m{\geq}0$, is then defined as follows:

$$H_p^m(C) = \left\{ \Phi \mid \sum_{\mathbf{k}\in\mathbb{Z}^2} c_{\mathbf{k}}^2 |\mathbf{k}|^{2m} < \infty \right\}. \tag{3}$$

Denoting zero mean functions from $H_p^m(C)$ by

$$H_p^m(C)/\mathbb{R} = \left\{ \Phi \in H_p^m(C) |\ c_{\mathbf{0}} = 0 \right\}, \tag{4}$$

it is easily shown that the $H^1(C)$ seminorm,

$$|\mathbf{\Phi}|_1 = (\nabla\Phi, \nabla\Phi)^{\frac{1}{2}}$$

(where $(\cdot,\cdot)$ denotes the usual L_2 inner product over C), provides a norm on $H_p^m(C)/\mathbb{R}$. Note that, denoting the dual space of $H_p^1(C)/\mathbb{R}$ by $H_p^{-1}(C)$, it follows that the definition of $H_p^m(C)/\mathbb{R}$ in (3) and (4) generalizes to the case $m{=}{-}1$ (in fact, it is valid for all $m{\in}\mathbb{R}$; see, e.g., Temam [13]).

The periodic Stokes problem (with viscosity set to unity) is formally stated below. Given a periodic vector field $\mathbf{f} \in [H_p^{-1}(C)/\mathbb{R}]^2$, the goal is to find $\mathbf{u}$ and p satisfying

$$-\Delta\mathbf{u} + \nabla p = \mathbf{f} \qquad \text{in C}, \tag{5}$$

$$\nabla\cdot\mathbf{u} = 0 \qquad \text{in C}, \tag{6}$$

together with boundary conditions

$$\mathbf{u}|_{\partial C_1} = \mathbf{u}|_{\partial C_3}, \quad \mathbf{u}|_{\partial C_2} = \mathbf{u}|_{\partial C_4} \qquad \text{and} \qquad p|_{\partial C_1} = p|_{\partial C_3}, \quad p|_{\partial C_2} = p|_{\partial C_4}. \tag{7}$$

The classical problem can be shown to be well posed by introducing the Fourier expansions for $\mathbf{u}$, p, and $\mathbf{f}$; see Temam [13, p. 9] for details.

A conventional weak formulation of (5)–(7) is the following. Given $\mathbf{f}{\in}[H_p^{-1}(C)/\mathbb{R}]^2$ the goal is to find $(\mathbf{u},p) \in [H_p^1(C)/\mathbb{R}]^2 \times (H_p^0(C)/\mathbb{R})$ such that

$$(\nabla\mathbf{u}, \nabla\mathbf{v}) - (p, \nabla\cdot\mathbf{v}) = (\mathbf{f}, \mathbf{v}) \qquad \forall \mathbf{v} \in [H_p^1(C)/\mathbb{R}]^2, \tag{8}$$

$$-(q, \nabla\cdot\mathbf{u}) = 0 \qquad \forall q \in H_p^0(C)/\mathbb{R}; \tag{9}$$

see Girault and Raviart [3]. We note that the stability of mixed formulations like (8)–(9) is a consequence of the LBB condition established by the following lemma.

LEMMA 2.1. $\exists\gamma > 0$ *such that*

$$\sup_{\mathbf{v}\in[H_p^1(C)/\mathbb{R}]^2} \frac{(q, \nabla\cdot\mathbf{v})}{|\mathbf{v}|_1} \geq \gamma\|q\|_0 \quad \forall q \in H_p^0(C)/\mathbb{R}.$$

Proof. Noting that

$$\begin{aligned} H_0^1(C) &= H_p^1(C)/\mathbb{R} \cap \left\{\mathbf{\Phi} \in H^1(C) | \mathbf{\Phi} = 0 \text{ on } \partial C\right\}, \\ L_0^2(C) &= H_p^0(C)/\mathbb{R}, \end{aligned}$$

we can appeal to the proof of Theorem 5.1 in [3, p. 80]; $\exists\gamma > 0$ such that

$$\sup_{\mathbf{v}\in[H_0^1(C)]^2} \frac{(q, \nabla\cdot\mathbf{v})}{|\mathbf{v}|_1} \geq \gamma\|q\|_0 \quad \forall q \in L_0^2(C).$$

Then since $H_0^1(C)\subset H_p^1(C)/\mathbb{R}$, we have that

$$\begin{aligned} \sup_{\mathbf{v}\in[H_p^1(C)/\mathbb{R}]^2} \frac{(q, \nabla\cdot\mathbf{v})}{|\mathbf{v}|_1} &\geq \sup_{\mathbf{v}\in[H_0^1(C)]^2} \frac{(q, \nabla\cdot\mathbf{v})}{|\mathbf{v}|_1} \\ &\geq \gamma\|q\|_0, \end{aligned}$$

where $L_0^2(C) = H_p^0(\Omega)/\mathbb{R}$.

Using a technique introduced by Stoyan [12] the quotient appearing in the LBB condition can be bounded from above by unity.

LEMMA 2.2.

$$\sup_{\mathbf{v}\in[H_p^1(C)/\mathbb{R}]^2} \frac{(q, \nabla\cdot\mathbf{v})}{|\mathbf{v}|_1\|q\|_0} \leq 1 \qquad \forall q \in H_p^0(C).$$

Proof. For any $q\in H_p^0(C)$ we have by the Cauchy–Schwarz inequality

$$\frac{(q, \nabla\cdot\mathbf{v})^2}{|\mathbf{v}|_1^2\|q\|_0^2} \leq \frac{\|q\|_0^2\|\nabla\cdot\mathbf{v}\|_0^2}{|\mathbf{v}|_1^2\|q\|_0^2}. \tag{10}$$

On noting the identity

$$(\nabla\mathbf{v}, \nabla\mathbf{w}) \equiv (\nabla\cdot\mathbf{v}, \nabla\cdot\mathbf{w}) + (\operatorname{rot}\mathbf{v}, \operatorname{rot}\mathbf{w}) \quad \forall\mathbf{v}, \mathbf{w} \in [H_p^1(C)/\mathbb{R}]^2,$$

we have that $|\mathbf{v}|_1^2\geq\|\nabla\cdot\mathbf{v}\|_0^2$, and hence from (10) we have

$$\sup_{\mathbf{v}\in[H_p^1(C)/\mathbb{R}]^2} \frac{(q, \nabla\cdot\mathbf{v})^2}{|\mathbf{v}|_1^2\|q\|_0^2} \leq 1. \qquad \square$$

This result will be seen to be useful later.

3. Q_1-Q_1 finite element approximation. Without loss of generality, here it may be assumed that L=1 with C=$[0, 1]\times[0, 1]$. Partitioning C into a mesh T_h of n^2 squares of side h=$1/n$, we take the standard bilinear finite element spaces for both velocity components and the pressure. More precisely, for each $T\in T_h$ we denote the

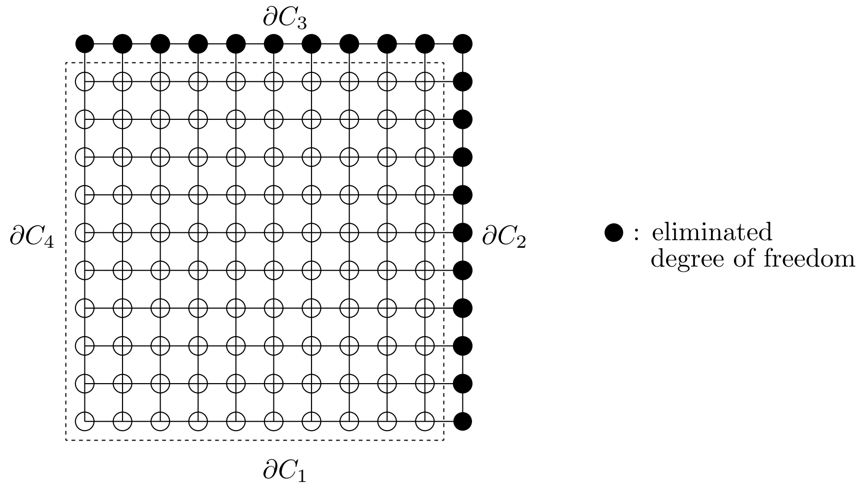

FIG. 1. *Periodic boundary conditions on a* $10{\times}10$ *mesh of* Q_1-Q_1 *elements.*

space of bilinear polynomials (linear in each coordinate direction) on T by $Q_1(T)$ and construct a pressure approximation space

$$Q_h = \left\{ q \in \mathcal{C}^0(C) : \ q|_T \in Q_1(T) \ \forall T \in T_h \right\} \cap H^1_p(C)$$

and a velocity space

$$V_h = Q_h \times Q_h.$$

The discrete formulation of (8)–(9) is as follows. Find $(\mathbf{u}_h, p_h) \in V_h \times Q_h$ such that

$$(\nabla \mathbf{u}_h, \nabla \mathbf{v}) - (p_h, \nabla \cdot \mathbf{v}) = (\mathbf{f}, \mathbf{v}) \qquad \forall \mathbf{v} \in V_h, \tag{11}$$

$$-(q, \nabla \cdot \mathbf{u}_h) = 0 \qquad \forall q \in Q_h. \tag{12}$$

The stability of (11)–(12) is governed by the following discrete LBB condition: we seek $\bar{\gamma}_h > 0$ such that

$$\sup_{\mathbf{v} \in V_h/\mathbb{R}^2} \frac{(\nabla \cdot \mathbf{v}, q)}{|\mathbf{v}|_1} \geq \bar{\gamma}_h \|q\|_0 \quad \forall q \in Q_h \tag{13}$$

and require that $\bar{\gamma}_h \geq \bar{\gamma}_* > 0$ as $h \to 0$. In the case of (nonperiodic) enclosed flow it is well known that the analogue of (13) is not uniformly satisfied with respect to the mesh parameter h (for uniform square grids $\bar{\gamma}_h = \mathcal{O}(h)$). We postpone discussion of the periodic case until the next section.

To solve a periodic Stokes flow problem starting from the standard finite element basis functions defined on the domain C, the periodic boundary conditions (7) must be used to eliminate the velocity and pressure degrees of freedom associated with nodes on the boundary segment $\partial C_2 \cup \partial C_3$ (see Figure 1), i.e., we need to ensure that $V_h \subset [H^1_p(C)]^2$ and $Q_h \subset H^0_p(C)$. In practice this may be achieved by combining rows and columns of the assembled finite element matrices; see Segal, Vuik, and Kassels [9] for details. The upshot is a block matrix system of the form

$$\begin{pmatrix} A & 0 & B_x^T \\ 0 & A & B_y^T \\ B_x & B_y & 0 \end{pmatrix} \begin{pmatrix} \mathbf{u}_x \\ \mathbf{u}_y \\ \mathbf{p} \end{pmatrix} = \begin{pmatrix} \mathbf{f}_x \\ \mathbf{f}_y \\ 0 \end{pmatrix}, \tag{14}$$

where the component matrices A (the discrete Laplacian operator), B_x, and B_y (which together form the discrete divergence operator) are *circulant* matrices. See Horn and Johnson [5, p. 20] for a summary of the properties of such matrices. We explore the eigenvalue spectrum of the matrices in (14) in the next section. At this point, we simply note that the matrices A, B_x, and B_y are all singular and have a zero eigenvalue corresponding to a nullspace consisting of constant vectors—this is a consequence of the fact that the requirement for uniqueness, i.e., $\mathbf{u}_h \in [H^1_p(C)/\mathbb{R}]^2$ and $p_h \in H^1_p(C)/\mathbb{R}$ is not explicity enforced in the construction of (14).

4. Fourier analysis of Q_1-Q_1. The LBB stability of Q_1-Q_1 in this periodic setting will now be assessed using discrete Fourier analysis. To this end, we note that after elimination of the $2n+1$ nodes on the boundary segment $\partial C_2 \cup \partial C_3$, we are left with a square mesh consisting of n^2 nodes (see Figure 1). If we label the remaining mesh points lexicographically, the discrete Fourier modes may be defined as follows:

$$\begin{gathered}\Psi^{i,j}(\boldsymbol{\theta}) = \exp\{\mathrm{i}(\theta_x i + \theta_y j)\}, \quad \mathrm{i} = \sqrt{-1}, \quad 0 \le i, j \le n-1, \\ \boldsymbol{\theta} = (\theta_x, \theta_y) \in \Theta_N = \left\{ \frac{2\pi}{n}(k,l) \ : -m \le (k,l) \le m+p \right\},\end{gathered} \tag{15}$$

where

$$m = \begin{cases} (n/2)-1 & \text{for n even,} \\ (n-1)/2 & \text{for n odd} \end{cases} \quad \text{and} \quad p = \begin{cases} 1 & \text{for n even,} \\ 0 & \text{for n odd.} \end{cases}$$

The set Θ_N is referred to as the wave number set and describes the $N{=}n^2$ frequencies that can be exhibited on an $n \times n$ mesh. Here we emphasize that Θ_N consists of wave numbers that take discrete values in the intervals

$$\begin{aligned} -\pi + \frac{2\pi}{n} \le (\theta_x, \theta_y) \le \pi, & \qquad n \text{ even}, \\ -\pi + \frac{\pi}{n} \le (\theta_x, \theta_y) \le \pi - \frac{\pi}{n}, & \qquad n \text{ odd}. \end{aligned}$$

The eigenvalues of the discrete Q_1 Laplacian matrix can now be identified.

LEMMA 4.1. *The n^2 eigenvalues of A arising in* (14) *are given by*

$$\Lambda_A(\boldsymbol{\theta}) = \frac{2}{3}(4 - \cos\theta_x - \cos\theta_y - 2\cos\theta_x \cos\theta_y), \quad \boldsymbol{\theta} \in \Theta_N. \tag{16}$$

Proof. The difference equation associated with the Q_1 discrete Laplacian on a uniform grid is the following:

$$\begin{aligned} Au_{i,j} = \frac{1}{3}(8u_{i,j} - (u_{i+1,j} + u_{i+1,j+1} + u_{i+1,j-1} + u_{i,j+1} \\ + u_{i,j-1} + u_{i-1,j+1} + u_{i-1,j} + u_{i-1,j-1})). \end{aligned} \tag{17}$$

Substituting the Fourier mode $\Psi^{i,j}(\boldsymbol{\theta})$ defined in (15) into (17) yields

$$\begin{aligned} A\Psi^{i,j} &= \tfrac{1}{3}\,(8 - (\Psi^{1,0} + \Psi^{1,1} + \Psi^{1,-1} + \Psi^{0,1} + \Psi^{0,-1} + \Psi^{-1,1} + \Psi^{-1,0} + \Psi^{-1,-1}))\Psi^{i,j} \\ &= \tfrac{1}{3}\,(8 - 2(\cos\theta_x + \cos\theta_y + \cos(\theta_x+\theta_y) + \cos(\theta_x - \theta_y)))\Psi^{i,j} \\ &= \tfrac{2}{3}\,(4 - \cos\theta_x - \cos\theta_y - 2\cos\theta_x\cos\theta_y)\Psi^{i,j}. \qquad \square \end{aligned}$$

COROLLARY 4.2. *The null space of A is one-dimensional, corresponding to the frequency $\boldsymbol{\theta}$=$\mathbf{0}$.*

Similarly, the difference equations corresponding to the matrices B_x, B_y in (14) are, respectively, given by

$$B_x u_{i,j} = \frac{h}{12}\left(4u_{i+1,j} - 4u_{i-1,j} + u_{i+1,j+1} - u_{i-1,j-1} + u_{i+1,j-1} - u_{i-1,j+1}\right),$$
$$B_y u_{i,j} = \frac{h}{12}\left(4u_{i,j+1} - 4u_{i,j-1} + u_{i+1,j+1} - u_{i-1,j-1} + u_{i-1,j+1} - u_{i+1,j-1}\right).$$

Moreover, applying the technique in Lemma 4.1 gives the eigenvalues.

LEMMA 4.3. *The n^2 eigenvalues of B_x and B_y are, respectively, given by*

$$\Lambda_{B_x}(\boldsymbol{\theta}) = \frac{\mathrm{i}h}{3}\sin\theta_x(\cos\theta_y + 2), \quad \boldsymbol{\theta} \in \Theta_N, \quad \text{and}$$
$$\Lambda_{B_y}(\boldsymbol{\theta}) = \frac{\mathrm{i}h}{3}\sin\theta_y(\cos\theta_x + 2), \quad \boldsymbol{\theta} \in \Theta_N. \tag{18}$$

The other discrete operator that arises in the discrete LBB stability condition (13) is the (pressure) mass matrix Q that is associated with the L_2 inner product over the space Q_h. An important point here is that the definition of the space Q_h ensures that Q is a circulant matrix—it is characterized by the following difference equation:

$$Qu_{i,j} = \frac{h^2}{36}\left(16u_{i,j} + 4u_{i+1,j} + 4u_{i-1,j} + 4u_{i,j+1} + 4u_{i,j-1} + u_{i+1,j+1} + u_{i+1,j-1} + u_{i-1,j+1} + u_{i-1,j-1}\right).$$

This means that the eigenvalues of Q can be explicitly identified.

LEMMA 4.4. *The n^2 eigenvalues of the pressure mass matrix Q are given by*

$$\Lambda_Q(\boldsymbol{\theta}) = \frac{h^2}{9}(\cos\theta_x + 2)(\cos\theta_y + 2), \quad \boldsymbol{\theta} \in \Theta_N. \tag{19}$$

The next lemma characterizes the LBB stability condition (13) in the form of a generalized eigenvalue problem.

LEMMA 4.5. *The discrete LBB constant $\bar{\gamma}_h$ associated with* (11)–(12) *is given by the square root of the smallest nonzero eigenvalue satisfying*

$$(B_x A^\dagger B_x^T + B_y A^\dagger B_y^T)\mathbf{p} = \lambda Q\mathbf{p}, \tag{20}$$

where $A^\dagger$ is the usual (Moore–Penrose) pseudoinverse of A.

Proof. Using Corollary 4.2 and the fact that A is square and symmetric, there exists a matrix $U \in \mathbb{R}^{n^2\times n^2}$ and diagonal matrix $\Sigma \in \mathbb{R}^{n^2\times n^2}$ such that $A = U\Sigma U^T$ with $U^T U = I$ and $\Sigma = \operatorname{diag}(\sigma_1, \sigma_2, \ldots, \sigma_{n^2-1}, 0)$. The pseudoinverse of A is defined by $A^\dagger = U\Sigma^\dagger U^T$, where $\Sigma^\dagger = \operatorname{diag}(1/\sigma_1, 1/\sigma_2, \ldots, 1/\sigma_{n^2-1}, 0)$. For the discrete LBB condition, we seek $\bar{\gamma}_h > 0$ such that for all $q \in Q_h$,

$$\begin{aligned}
\bar{\gamma}_h \|q\|_0 &\le \sup_{\mathbf{v}\in V_h/\mathbb{R}^2} \frac{(q, \nabla\cdot\mathbf{v})}{|\mathbf{v}|_1} \\
&= \max_{\mathbf{v}_x,\mathbf{v}_y \notin \mathrm{Null}(A)} \frac{\mathbf{v}_x^T B_x^T \mathbf{q} + \mathbf{v}_y^T B_y^T \mathbf{q}}{\left(\mathbf{v}_x^T A \mathbf{v}_x + \mathbf{v}_y^T A \mathbf{v}_y\right)^{\frac{1}{2}}} \\
&= \max_{\mathbf{z}_x,\mathbf{z}_y \notin \mathrm{Null}((A^\dagger)^{\frac{1}{2}} A (A^\dagger)^{\frac{1}{2}})} \frac{\mathbf{z}_x^T (A^\dagger)^{\frac{1}{2}} B_x^T \mathbf{q} + \mathbf{z}_y^T (A^\dagger)^{\frac{1}{2}} B_y^T \mathbf{q}}{(\mathbf{z}_x^T (A^\dagger)^{\frac{1}{2}} A (A^\dagger)^{\frac{1}{2}} \mathbf{z}_x + \mathbf{z}_y^T (A^\dagger)^{\frac{1}{2}} A (A^\dagger)^{\frac{1}{2}} \mathbf{z}_y)^{\frac{1}{2}}}.
\end{aligned} \tag{21}$$

Here we have made the change of variable $\mathbf{v}_x = (A^\dagger)^{\frac{1}{2}}\mathbf{z}_x$ and $\mathbf{v}_y = (A^\dagger)^{\frac{1}{2}}\mathbf{z}_y$, where $(A^\dagger)^{\frac{1}{2}} = U(\Sigma^\dagger)^{\frac{1}{2}}U^T$ and $(\Sigma^\dagger)^{\frac{1}{2}} = \mathrm{diag}(1/\sqrt{\sigma_1}, 1/\sqrt{\sigma_2}, \ldots, 1/\sqrt{\sigma_{n^2-1}}, 0)$. We note that the first n^2-1 columns $\{\mathbf{u}_i\}_{i=1}^{n^2-1}$ of U, say, $\bar{U}$, form a basis for $\mathbb{R}^{n^2}\backslash\mathrm{Null(A)}$. Also $\mathbf{z}_x, \mathbf{z}_y \in \mathrm{span}\,\{\mathbf{u}_i\}_{i=1}^{n^2-1}$ and

$$
\begin{aligned}
(A^\dagger)^{\frac{1}{2}}A(A^\dagger)^{\frac{1}{2}} &= U(\Sigma^\dagger)^{\frac{1}{2}}U^T U\Sigma U^T U(\Sigma^\dagger)^{\frac{1}{2}}U^T \\
&= U\mathrm{diag}\,(1,1,\ldots,1,0)\,U^T = \bar{U}I_{n^2-1}\bar{U}^T.
\end{aligned}
$$

Writing $\mathbf{z}_x = \sum_{i=1}^{n^2-1}\alpha_i\mathbf{u}_i$, for some real coefficients $\{\alpha_i\}_{i=1}^{n^2-1}$, we have that

$$
\mathbf{z}_x^T(A^\dagger)^{\frac{1}{2}}A(A^\dagger)^{\frac{1}{2}}\mathbf{z}_x = \left(\sum_{i=1}^{n^2-1}\alpha_i\mathbf{u}_i\right)^T \bar{U}I_{n^2-1}\bar{U}^T\left(\sum_{i=1}^{n^2-1}\alpha_i\mathbf{u}_i\right) = \sum_{i=1}^{n^2-1}\alpha_i^2 = \mathbf{z}_x^T\mathbf{z}_x.
$$

Thus

$$
\begin{aligned}
\sup_{\mathbf{v}\in V_h/\mathbb{R}^2}\frac{(q,\nabla\cdot\mathbf{v})}{|\mathbf{v}|_1} &= \max_{\mathbf{z}_x,\mathbf{z}_y}\frac{\mathbf{z}_x^T(A^\dagger)^{\frac{1}{2}}B_x^T\mathbf{q} + \mathbf{z}_y^T(A^\dagger)^{\frac{1}{2}}B_y^T\mathbf{q}}{\left(\mathbf{z}_x^T\mathbf{z}_x + \mathbf{z}_y^T\mathbf{z}_y\right)^{\frac{1}{2}}} \\
&= \left[\mathbf{q}^T(B_xA^\dagger B_x^T + B_yA^\dagger B_y^T)\mathbf{q}\right]^{\frac{1}{2}},
\end{aligned}
$$

and hence $\bar{\gamma}_h$ is characterized by

$$
\bar{\gamma}_h^2 = \min_{\mathbf{q}\in\mathbb{R}^{n^2}}\frac{\mathbf{q}^T(B_xA^\dagger B_x^T + B_yA^\dagger B_y^T)\mathbf{q}}{\mathbf{q}^TQ\mathbf{q}}. \qquad \square
$$

The following lemma provides a sharp upper bound on the eigenvalues satisfying (20).

LEMMA 4.6. *The maximum eigenvalue λ_{max} of* (20) *satisfies $\lambda_{max} \le 1$.*

Proof. Since $Q_h \subset H_p^1(C) \subset H_p^0(C)$, then for any $q_h \in Q_h$, we can apply Lemma 2.2:

$$
\sup_{\mathbf{v}\in[H_p^1(C)/\mathbb{R}]^2}\frac{(q_h,\nabla\cdot\mathbf{v})^2}{|\mathbf{v}|_1^2\|q_h\|_0^2} \le 1.
$$

Also, since $V_h/\mathbb{R}^2 \subset [H_p^1(C)/\mathbb{R}]^2$ we have that

$$
\begin{aligned}
1 \ge \max_{q_h\in Q_h}\sup_{\mathbf{v}\in[H_p^1(C)/\mathbb{R}]^2}\frac{(q_h,\nabla\cdot\mathbf{v})^2}{|\mathbf{v}|_1^2\|q_h\|_0^2} &\ge \max_{q_h\in Q_h}\max_{\mathbf{v}_h\in V_h/\mathbb{R}^2}\frac{(q_h,\nabla\cdot\mathbf{v}_h)^2}{|\mathbf{v}_h|_1^2\|q_h\|_0^2} \\
&= \max_{\mathbf{q}\in\mathbb{R}^{n^2}}\frac{\mathbf{q}^T(B_xA^\dagger B_x^T + B_yA^\dagger B_y^T)\mathbf{q}}{\mathbf{q}^TQ\mathbf{q}} \\
&= \lambda_{max}. \qquad \square
\end{aligned}
$$

The next lemma relates the LBB eigenvalue problem to the eigenvalues of the component matrices in (14). Specifically, eigenvalues of (20) are a simple combination of the eigenvalues of A, B_x, B_y and the mass matrix Q.

LEMMA 4.7. *The LBB eigenvalue problem* (20) *simplifies to*

$$
(\Sigma_Q)^{-1}(\Sigma_A)^\dagger(\Sigma_{B_x}^H\Sigma_{Bx} + \Sigma_{By}^H\Sigma_{By})\mathbf{q} = \lambda\mathbf{q},
$$

where Σ_M denotes a diagonal matrix whose entries are the eigenvalues of M. M^H denotes the conjugate transpose of M.

Proof. As is evident in establishing the results (16), (18), and (19), A, B_x, B_y, and Q share the same set of eigenvectors $\left\{\Psi_{\boldsymbol{\theta}}\right\}_{\boldsymbol{\theta}\in\Theta_N}$ so that for each $\boldsymbol{\theta}\in\Theta_N$, $\Psi_{\boldsymbol{\theta}}\in\mathbb{C}^{\,n^2\times 1}$ has entries defined by

$$\left[\Psi_{\boldsymbol{\theta}}\right]_{\mathcal{G}(i,j)} = \exp\left\{\mathrm{i}(\theta_x i + \theta_y j)\right\}, \quad 0 \le (i,j) \le n-1,$$

where $\mathcal{G}(i,j)$ denotes the lexicographical numbering of the mesh points. Thus, the Fourier matrix

$$U = \frac{1}{n}\left[\Psi_{\boldsymbol{\theta}_1}, \Psi_{\boldsymbol{\theta}_2}, \ldots, \Psi_{\boldsymbol{\theta}_{n^2}}\right] \in \mathbb{C}^{\,n^2\times n^2}$$

satisfies

$$\begin{aligned} U^H A U = \Sigma_A, &\quad U^H Q U = \Sigma_Q,\\ U^H B_x U = \Sigma_{B_x}, &\quad U^H B_y U = \Sigma_{B_y},\\ U^H &= U^{-1}. \end{aligned}$$

Applying a similarity transformation to (20) yields

$$\begin{aligned} \lambda \Sigma_Q U^H \mathbf{q} &= U^H \left(B_x A^\dagger B_x^T + B_y A^\dagger B_y^T\right) U U^H \mathbf{q}\\ &= \left(U^H B_x A^\dagger B_x^T U + U^H B_y A^\dagger B_y^T U\right) U^H \mathbf{q}. \end{aligned}$$

Setting $\bar{\mathbf{q}}$=$U^H\mathbf{q}$,

$$\begin{aligned} \lambda \Sigma_Q \bar{\mathbf{q}} &= \left(U^H B_x U (\Sigma_A)^\dagger U^H B_x^T U + U^H B_y U (\Sigma_A)^\dagger U^H B_y^T U\right) \bar{\mathbf{q}}\\ &= \left(\Sigma_{B_x} (\Sigma_A)^\dagger U^H B_x^T U + \Sigma_{B_y} (\Sigma_A)^\dagger U^H B_y^T U\right) \bar{\mathbf{q}}\\ &= \left((\Sigma_A)^\dagger \Sigma_{B_x} \Sigma_{B_x}^H + (\Sigma_A)^\dagger \Sigma_{B_y} \Sigma_{B_y}^H\right) \bar{\mathbf{q}}. \end{aligned}$$

Therefore

$$\Sigma_Q^{-1} (\Sigma_A)^\dagger \left(\Sigma_{B_x}^H \Sigma_{B_x} + \Sigma_{B_y}^H \Sigma_{B_y}\right) \bar{\mathbf{q}} = \lambda \bar{\mathbf{q}}. \qquad \square$$

We summarize the main result of the section in the following theorem.

THEOREM 4.8. *On an $n \times n$ mesh the n^2 eigenvalues $\Lambda_{lbb}(\boldsymbol{\theta})$ of (20) satisfy*

$$\Lambda_{lbb}(\boldsymbol{\theta}) = \frac{3\left[\sin^2\theta_x(\cos\theta_y + 2)^2 + \sin^2\theta_y(\cos\theta_x + 2)^2\right]}{2(4 - \cos\theta_x - \cos\theta_y - 2\cos\theta_x\cos\theta_y)(\cos\theta_y + 2)(\cos\theta_x + 2)},$$

$$\boldsymbol{\theta} \in \Theta_N. \tag{22}$$

Proof. From Lemma 4.7 we may write

$$\Lambda_{lbb}(\boldsymbol{\theta}) = \frac{|\Lambda_{B_x}(\boldsymbol{\theta})|^2 + |\Lambda_{B_y}(\boldsymbol{\theta})|^2}{\Lambda_A(\boldsymbol{\theta})\Lambda_Q(\boldsymbol{\theta})}, \quad \boldsymbol{\theta} \in \Theta_N. \tag{23}$$

Substituting (16), (18), and (19) into (23) gives the result. $\square$

The surface generated by plotting $\Lambda_{lbb}(\boldsymbol{\theta})$ over $[-\pi,\pi]^2$ is illustrated in Figure 2. We shall refer to this surface as S_{lbb}. It can be seen that there appears to be eight

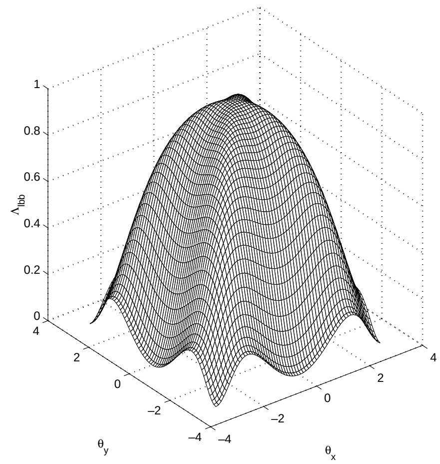

FIG. 2. *The LBB eigenvalue surface.*

points where S_{lbb} vanishes. The maximum value of S_{lbb} also appears to be unity. The following lemmas confirm these observations.

LEMMA 4.9.

$$\lim_{\boldsymbol{\theta}\to\mathbf{0}} S_{lbb}(\boldsymbol{\theta}) = 1.$$

Proof. We use an argument based on l'Hôpital's rule and write

$$S_{lbb}(\boldsymbol{\theta}) = \frac{3f(\boldsymbol{\theta})}{2g(\boldsymbol{\theta})},$$

where

$$\begin{aligned} f(\boldsymbol{\theta}) &= \sin^2\theta_x(\cos\theta_y+2)^2 + \sin^2\theta_y(\cos\theta_x+2)^2, \\ g(\boldsymbol{\theta}) &= (\cos\theta_y+2)(\cos\theta_x+2)(4-\cos\theta_x-2\cos\theta_y\cos\theta_x-\cos\theta_y). \end{aligned}$$

Expanding f and g using Taylor series about $\boldsymbol{\theta}$=$\mathbf{0}$, we have

$$\lim_{\boldsymbol{\theta}\to\mathbf{0}} S_{lbb}(\boldsymbol{\theta}) = \frac{3}{2}\lim_{\mathbf{h}\to\mathbf{0}} \frac{f(\mathbf{0}) + \mathbf{h}\cdot\nabla f|_{\boldsymbol{\theta}=\mathbf{0}} + \frac{1}{2}\mathbf{h}^T(\mathcal{H}f)\mathbf{h}|_{\boldsymbol{\theta}=\mathbf{0}} + \mathcal{O}(\mathbf{h}^3)}{g(\mathbf{0}) + \mathbf{h}\cdot\nabla g|_{\boldsymbol{\theta}=\mathbf{0}} + \frac{1}{2}\mathbf{h}^T(\mathcal{H}g)\mathbf{h}|_{\boldsymbol{\theta}=\mathbf{0}} + \mathcal{O}(\mathbf{h}^3)}, \tag{24}$$

where $\mathcal{H}$ is the Hessian matrix.

Since $S_{lbb}(\boldsymbol{\theta})$ is locally symmetric about $\boldsymbol{\theta}$=$\mathbf{0}$, $\lim_{\boldsymbol{\theta}\to\mathbf{0}}\Lambda_{lbb}(\boldsymbol{\theta})$ is invariant of the direction that the limit is taken from. Therefore to simplify matters we may take $\mathbf{h}$=$(h,0)$ in (24). Calculating derivatives we have

$$\begin{aligned} \frac{\partial f}{\partial\theta_x} &= 2\sin\theta_x\cos\theta_x(\cos\theta_y+2)^2 - 2\sin^2\theta_y\sin\theta_x(\cos\theta_x+2), \\ \frac{\partial^2 f}{\partial\theta_x^2} &= 2\cos^2\theta_x(\cos\theta_y+2)^2 - 2\sin^2\theta_x(\cos\theta_y+2)^2 \\ &\qquad +2\sin^2\theta_y\sin^2\theta_x - 2\sin^2\theta_y\cos\theta_x(\cos\theta_x+2), \\ \frac{\partial g}{\partial\theta_x} &= \sin\theta_x(\cos\theta_y+2)(4\cos\theta_x\cos\theta_y+5\cos\theta_y+2\cos\theta_x-2), \end{aligned}$$

$$\frac{\partial^2 g}{\partial \theta_x^2} = \cos\theta_x(\cos\theta_y+2)(4\cos\theta_x\cos\theta_y+5\cos\theta_y+2\cos\theta_x-2) \\ -\sin\theta_x(\cos\theta_y+2)(4\sin\theta_x\cos\theta_y+2\sin\theta_x).$$

It is clear that $f(\mathbf{0})=0$, $g(\mathbf{0})=0$, with

$$\frac{\partial f}{\partial \theta_x}|_{\boldsymbol{\theta}=\mathbf{0}} = 0 \quad \text{and} \quad \frac{\partial g}{\partial \theta_x}|_{\boldsymbol{\theta}=\mathbf{0}} = 0.$$

Therefore

$$\lim_{\boldsymbol{\theta}\to\mathbf{0}} S_{lbb}(\boldsymbol{\theta}) = \frac{3}{2}\lim_{h\to 0}\frac{\frac{1}{2}h^2\frac{\partial^2 f}{\partial x^2}+\mathcal{O}(h^3)}{\frac{1}{2}h^2\frac{\partial^2 g}{\partial x^2}+\mathcal{O}(h^3)} = \frac{3}{2}\times\frac{18}{27} = 1. \qquad \square$$

Lemma 4.10.

$$S_{lbb}(\boldsymbol{\phi}) = 0 \quad \textit{for } \boldsymbol{\phi}\in\{\pm(\pi,\pi),\pm(\pi,-\pi),\pm(\pi,0),\pm(0,\pi)\}.$$

Proof. Putting $\Lambda_{lbb}=0$ from (22) gives

$$\sin^2\theta_x(2+\cos\theta_y)^2 = 0 \qquad \text{and} \qquad \sin^2\theta_y(2+\cos\theta_x)^2 = 0.$$

Since the bracketed terms are strictly positive this implies that

$$\sin\theta_x = 0 = \sin\theta_y.$$

On noting that $\lim_{\boldsymbol{\theta}\to\mathbf{0}}S_{lbb}(\boldsymbol{\theta})=1$, by Lemma 4.9, we arrive at the desired result. $\square$

Remark 4.1. *From Lemma* 4.10 *we see that for n even, the discrete divergence operator in* (14)*, $B=[B_x,B_y]$, is rank deficient by three. On the other hand, for n odd, B is of full rank.*

To complete our discussion in this section we show that the Q_1-Q_1 approximation is unstable in the sense that the discrete LBB constant tends to zero as h tends to zero.

Lemma 4.11. *There exists $\boldsymbol{\theta}^h\in\Theta_N$ such that $\Lambda_{lbb}(\boldsymbol{\theta}^h)=\mathcal{O}(h^2)$.*

Proof. We consider the case of n even and set $\boldsymbol{\theta}^h=\boldsymbol{\theta}^s+\mathbf{h}$, where $\boldsymbol{\theta}^s=(-\pi,-\pi)$ and $\mathbf{h}=(h,h)=(\frac{2\pi}{n},\frac{2\pi}{n})$.[1] As in the proof of Lemma 4.9 we expand the numerator and denominator of S_{lbb} using Taylor series about $\boldsymbol{\theta}^s$. Since we are expanding in the direction $\theta_x=\theta_y$ we may parameterize both f and g (see the proof of Lemma 4.9) and write

$$f(\theta_x,\theta_y) = f(\theta_x,\theta_x), \\ g(\theta_x,\theta_y) = g(\theta_x,\theta_x) \quad \text{along } \theta_x=\theta_y.$$

Thus,

$$S_{lbb}(\boldsymbol{\theta}^s+\mathbf{h}) = \frac{f(-\pi,-\pi)+2h\frac{\partial f}{\partial\theta_x}|_{\theta_x=-\pi}+h^2\frac{\partial^2 f}{\partial\theta_x^2}|_{\theta_x=-\pi}+\mathcal{O}(h^3)}{g(-\pi,-\pi)+2h\frac{\partial g}{\partial\theta_x}|_{\theta_x=-\pi}+h^2\frac{\partial^2 g}{\partial\theta_x^2}|_{\theta_x=-\pi}+\mathcal{O}(h^3)}. \tag{25}$$

Evaluating the various terms in (25) yields

$$S_{lbb}(\boldsymbol{\theta}^h) = S_{lbb}(\theta^s+\mathbf{h}) = \frac{2h^2}{4+\mathcal{O}(h^2)} \le \frac{1}{2}h^2.$$

Finally, since $\boldsymbol{\theta}^h\in\Theta_N$ we have $\Lambda_{lbb}(\boldsymbol{\theta}^h)\le\frac{1}{2}h^2$. $\square$

[1] In the case when n is odd we may take $\mathbf{h}=(\frac{\pi}{n},\frac{\pi}{n})$.

5. Stabilization of the discrete formulation. We now consider a stabilized version of the discrete formulation (12) that is analogous to the method introduced by Brezzi and Pitkäranta [1] and developed by Brezzi and Douglas [2]. A consistent implementation (having a nonzero right-hand side) was introduced by Hughes, Franca, and Balestra [6].

Find $(\mathbf{u}_h, p_h) \in V_h \times Q_h$ such that

$$(\nabla \mathbf{u}_h, \nabla \mathbf{v}) - (p_h, \nabla \cdot \mathbf{v}) = (\mathbf{f}, \mathbf{v}) \qquad \forall \mathbf{v} \in V_h, \tag{26}$$

$$-(q, \nabla \cdot \mathbf{u}_h) - \beta C_h(p_h, q) = 0 \qquad \forall q \in Q_h, \tag{27}$$

where $\beta > 0$ is the stabilization parameter and

$$C_h(p_h, q) = h^2 \sum_{T \in T_h} \int_T \nabla p_h \cdot \nabla q \ \mathrm{dT} \qquad \text{for } p_h, q \in Q_h \subset H_p^1(C)$$

is the stabilization operator.

A crucial point here is that the stabilization operator is defined on a periodic (pressure) space, so the corresponding stabilization matrix is the scaled discrete Q_1 Laplacian with periodic boundary conditions. Specifically, the stabilized matrix problem is

$$\begin{pmatrix} A & 0 & B_x^T \\ 0 & A & B_y^T \\ B_x & B_y & -\beta h^2 A \end{pmatrix} \begin{pmatrix} \mathbf{u}_x \\ \mathbf{u}_y \\ \mathbf{p} \end{pmatrix} = \begin{pmatrix} \mathbf{f}_x \\ \mathbf{f}_y \\ 0 \end{pmatrix} \tag{28}$$

(cf. (14)) and the corresponding (stabilized) LBB eigenvalue problem is given by

$$(B_x A^\dagger B_x^T + B_y A^\dagger B_y^T + \beta h^2 A)\mathbf{q} = \lambda Q \mathbf{q}. \tag{29}$$

The following theorem is immediate.

THEOREM 5.1. *On an $n \times n$ mesh the n^2 eigenvalues of* (29) *are given by*

$$\Lambda(\boldsymbol{\theta}, \beta) = \Lambda_{lbb}(\boldsymbol{\theta}) + \beta\, \Lambda_{stab}(\boldsymbol{\theta}) \quad \forall \boldsymbol{\theta} \in \Theta_N, \tag{30}$$

where $\Lambda_{lbb}(\boldsymbol{\theta})$ is given by (22) *and*

$$\Lambda_{stab}(\boldsymbol{\theta}) = 6 \frac{(4 - \cos\theta_x - \cos\theta_y - 2\cos\theta_x \cos\theta_y)}{(\cos\theta_x + 2)(\cos\theta_y + 2)}. \tag{31}$$

Proof. The generalized eigenvalue problem (29) diagonalizes to

$$\left[\Sigma_Q^{-1} \Sigma_A^\dagger (\Sigma_{B_x}^H \Sigma_{Bx} + \Sigma_{By}^H \Sigma_{By}) + \beta h^2 \Sigma_Q^{-1} \Sigma_A\right] \mathbf{q} = \lambda \mathbf{q}.$$

Substituting in the eigenvalue expressions for A,B_x, B_y and Q yields (30)–(31). ◻

Figures 3–5 give an illustration of how the stabilized LBB surface evolves as β is increased. For a given frequency $\boldsymbol{\theta}$, (30) describes $\Lambda(\boldsymbol{\theta})$ as a continuous linear function in β. The rate at which this linear function grows is determined by the specific value of $\Lambda_{stab}(\boldsymbol{\theta})$. Denoting the surface generated by $\Lambda_{stab}(\boldsymbol{\theta})$ when $\boldsymbol{\theta}$ is allowed to range over $[-\pi, \pi]^2$, by $S_{stab}(\boldsymbol{\theta})$, the eigenvalues that evolve the fastest and the slowest are characterized by the following lemma.

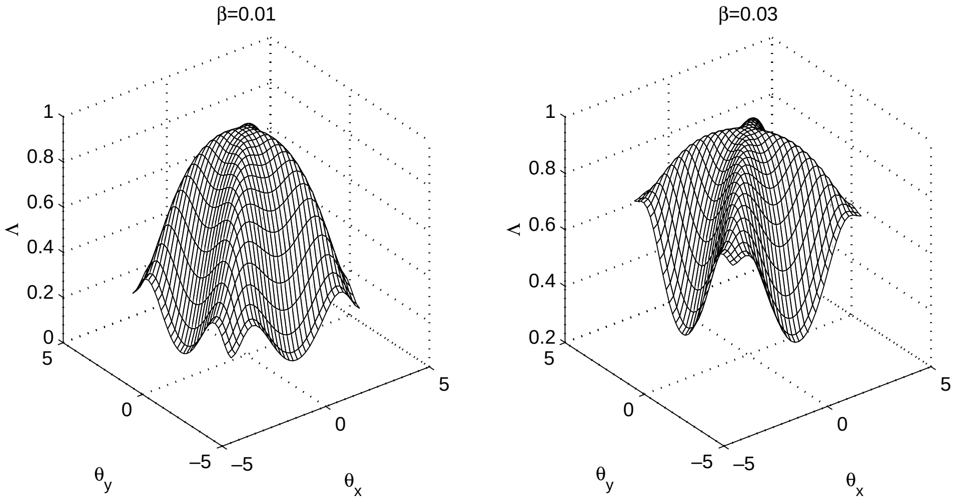

FIG. 3. *Stabilized LBB surface for* $\beta = 0.01$ *and* $\beta = 0.03$.

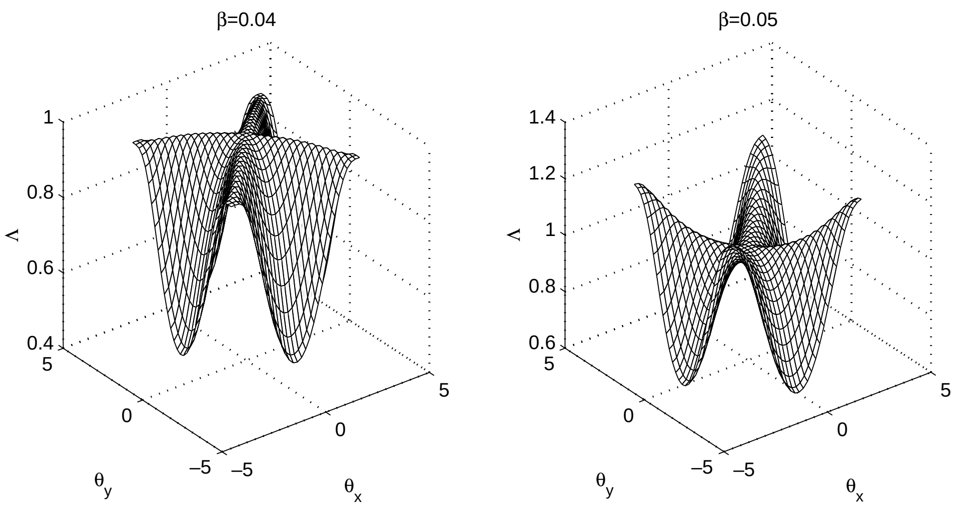

FIG. 4. *Stabilized LBB surface for* $\beta = 0.04$ *and* $\beta = 0.05$.

LEMMA 5.2.

$$S_{stab}(\boldsymbol{\theta}^{\star}) = \max_{\boldsymbol{\theta}\in[-\pi,\pi]^2} S_{stab}(\boldsymbol{\theta}) = 24,$$

where

$$\boldsymbol{\theta}^{\star} = \pm(\pi,\pi) \ \textit{or} \ \pm(\pi,-\pi)$$

and

$$S_{stab}(\mathbf{0}) = \min_{\boldsymbol{\theta}\in[-\pi,\pi]^2} S_{stab}(\boldsymbol{\theta}) = 0.$$

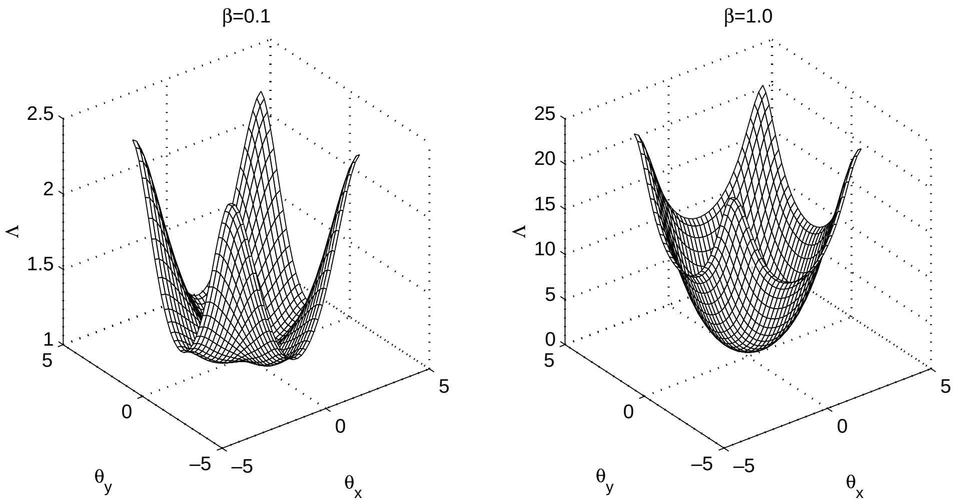

FIG. 5. *Stabilized LBB surface for $\beta = 0.1$ and $\beta = 1$.*

Proof. The stationary conditions are

$$\frac{\partial S_{stab}}{\partial \theta_x} = 0 \quad \text{and} \quad \frac{\partial S_{stab}}{\partial \theta_y} = 0,$$

which implies

$$\sin\theta_x = 0 = \sin\theta_y, \tag{32}$$

which has the solutions (θ_x, θ_y)=$(0, 0)$,$(\pm\pi, 0)$, $(0, \pm\pi)$,$\pm(\pi, \pi)$, and $\pm(\pi, -\pi)$. By simply substituting these stationary points back into the expression for $S_{stab}(\boldsymbol{\theta})$, we can explicitly see that $\pm(\pi, \pi)$ and $\pm(\pi, -\pi)$ are the (global) maxima of $S_{stab}(\boldsymbol{\theta})$ with $S_{stab}(\boldsymbol{\theta}^\star)$=24. Likewise it can be seen that $\boldsymbol{\theta}$=$(0, 0)$ is in fact the global minimum of $S_{stab}(\boldsymbol{\theta})$ with $S_{stab}(\mathbf{0})$=0. ◻

We now let $\boldsymbol{\theta}$ range over $[-\pi, \pi]^2$ and denote the surface generated by $\Lambda(\boldsymbol{\theta}, \beta)$ by $\mathcal{S}(\boldsymbol{\theta}, \beta)$, i.e.,

$$\mathcal{S}(\boldsymbol{\theta}, \beta) = S_{lbb}(\boldsymbol{\theta}) + \beta S_{stab}(\boldsymbol{\theta}).$$

(Typical examples are plotted in Figures 3–5.) Lemmas 4.9 and 5.2 imply that the eigenvalue $\mathcal{S}(\mathbf{0}, \beta)$ equals unity for all values of β. Moreover, using Lemma 4.10, we see that $\boldsymbol{\theta}^\star \in S$, and hence the fastest evolving eigenvalue with respect to the stabilization parameter is of the form $\mathcal{S}(\boldsymbol{\theta}^\star, \beta)$=$24\beta$ and is of multiplicity four.

LEMMA 5.3. *Let*

$$\mathcal{S}_{max}(\beta) = \max_{\boldsymbol{\theta}\in[-\pi,\pi]^2} \{\mathcal{S}(\boldsymbol{\theta}, \beta)\}.$$

Then,

(i) $\mathcal{S}_{max}(\beta) = 1 \quad \beta \leq \frac{1}{24}$,

(ii) $\mathcal{S}_{max}(\beta) = \mathcal{S}(\boldsymbol{\theta}^\star) \quad \beta \geq \frac{1}{24}$,

where $\boldsymbol{\theta}^\star$ is given by Lemma 5.2.

Proof. (i) We first examine the case when β=0. By Lemmas 4.6 and 4.9 we have that

$$\mathcal{S}_{max}(0) = \max_{\boldsymbol{\theta}\in[-\pi,\pi]^2} (\mathcal{S}(\boldsymbol{\theta},0)) = \max_{\boldsymbol{\theta}\in[-\pi,\pi]^2} (S_{lbb}(\boldsymbol{\theta})) = S_{lbb}(\mathbf{0}) = 1.$$

Furthermore, from Lemma 5.2 the eigenvalue $\mathcal{S}(\mathbf{0},\beta)$ is stationary at unity as β is increased from zero. Since $\mathcal{S}_{stab}(\boldsymbol{\theta})>0$ for all $\boldsymbol{\theta} \in [-\pi,\pi]^2\setminus\{\mathbf{0}\}$, each eigenvalue $\mathcal{S}_{\boldsymbol{\theta}}(\beta)=\mathcal{S}(\boldsymbol{\theta},\beta)$, $\boldsymbol{\theta} \in [-\pi,\pi]^2\setminus\{\mathbf{0}\}$, increases linearly from some point $\mathcal{S}(\boldsymbol{\theta},0)<1$ towards unity, that is, for a given $\boldsymbol{\theta} \in [-\pi,\pi]^2\setminus\{\mathbf{0}\}$

$$\frac{\partial \mathcal{S}_{\boldsymbol{\theta}}}{\partial\beta} = \mathcal{S}_{stab}(\boldsymbol{\theta}) > 0 \quad \text{and} \quad \mathcal{S}_{\boldsymbol{\theta}}(0) < 1 \quad \forall \boldsymbol{\theta} \in [-\pi,\pi]^2\setminus\{\mathbf{0}\}\,.$$

We now determine the first instance when an eigenvalue coincides with the stationary eigenvalue at unity. To this end we let

$$\mathcal{B}^\star = \left\{\beta \ : \ \mathcal{S}_{\boldsymbol{\theta}}(\beta) = 1, \ \boldsymbol{\theta} \in [-\pi,\pi]^2\setminus\{\mathbf{0}\}\right\};$$

denote the set of stabilization parameter values at which each eigenvalue coincides with unity. Notice that

$$\beta \in \mathcal{B}^\star \iff \beta = \frac{1 - S_{lbb}(\boldsymbol{\phi})}{S_{stab}(\boldsymbol{\phi})} \quad \text{for some } \boldsymbol{\phi} \in [-\pi,\pi]^2\setminus\{\mathbf{0}\}.$$

We now define $\beta^\star$ to be the smallest value of β for which some eigenvalue attains the value unity. Thus $\beta^\star$ is given by

$$\beta^\star = \mathrm{glb}\,(\mathcal{B}^\star) = \min_{\boldsymbol{\theta}\in[-\pi,\pi]^2\setminus\{\mathbf{0}\}} \frac{1 - S_{lbb}(\boldsymbol{\theta})}{S_{stab}(\boldsymbol{\theta})}. \tag{33}$$

Calculating the stationary points of the quotient in (33) results in the conditions

$$\frac{3\sin\theta_x(\cos\theta_y+2)(\cos\theta_y-1)(\cos\theta_y-\cos\theta_x)}{2(4-\cos\theta_x-2\cos\theta_x\cos\theta_y-\cos\theta_y)^3} = 0$$

and

$$\frac{3\sin\theta_y(\cos\theta_x+2)(\cos\theta_x-1)(\cos\theta_x-\cos\theta_y)}{2(4-\cos\theta_x-2\cos\theta_x\cos\theta_y-\cos\theta_y)^3} = 0,$$

giving the solutions $\boldsymbol{\theta}=\pm(\alpha,0),\pm(0,\alpha)$ and $(\alpha,\pm\alpha)$ for any $\alpha\in[-\pi,\pi]^2\setminus\{\mathbf{0}\}$. By substituting back into the quotient in (33) we see that the solutions of the form $\boldsymbol{\theta}=(\alpha,\pm\alpha)$ are global minima with $\beta^\star=\frac{1}{24}$. This completes the proof of (i). On noting that $\boldsymbol{\theta}^\star$ (the fastest growing eigenvalue w.r.t. β) is of the form $(\alpha,\pm\alpha)$ we deduce that $\mathcal{S}_{max}(\beta)=\mathcal{S}_{\boldsymbol{\theta}^\star}(\beta)$ for $\beta\geq\frac{1}{24}$ by Lemma 5.2. ∎

LEMMA 5.4. *Let*

$$\mathcal{S}_{min}(\beta) = \min_{\boldsymbol{\theta}\in[-\pi,\pi]^2} \{\mathcal{S}(\boldsymbol{\theta},\beta)\}\,.$$

Then,

(i) $\mathcal{S}_{min}(\beta) = \mathcal{S}(\boldsymbol{\theta}^+,\beta)$; $\quad \beta \leq \frac{1}{12}$, *where* $\boldsymbol{\theta}^+=(0,\pm\pi)$ *or* $(\pm\pi,0)$,

(ii) $\mathcal{S}_{min}(\beta) = 1$; $\quad \beta \geq \frac{1}{12}$.

Proof. Returning to the proof of Lemma 5.3, we saw that $(0, \pm\alpha)$ and $(\pm\alpha, 0)$ are stationary points of the quotient given in (33). On further inspection it can be seen that these points are in fact global maxima with

$$\frac{1 - \mathcal{S}_{lbb}(\boldsymbol{\phi})}{\mathcal{S}_{stab}(\boldsymbol{\phi})} = \frac{1}{12}; \qquad \boldsymbol{\phi} = (0, \pm\alpha) \text{ or } (\pm\alpha, 0).$$

Consequently $\mathrm{lub}(\mathcal{B}^\star) = 1/12$. Thus, the last eigenvalues to coincide with unity do so when $\beta{=}\frac{1}{12}$ and are given by $\mathcal{S}(\boldsymbol{\phi}, \beta)$ (where $\boldsymbol{\phi}{=}(0, \pm\alpha)$ or $(\pm\alpha, 0)$). Notice that $\boldsymbol{\theta}^+$ is of the form $(0, \pm\alpha)$ or $(\pm\alpha, 0)$. Moreover, at $\beta{=}0$, $\mathcal{S}(\boldsymbol{\theta}^+, 0){=}0$ by Lemma 4.10. Therefore we must have that $\mathcal{S}_{min}(\beta){=}\mathcal{S}(\boldsymbol{\theta}^+, \beta)$ for $\beta{\le}\frac{1}{12}$. This proves (i). Since $\mathcal{S}(\boldsymbol{\theta}^+, \beta)$ is the last eigenvalue to coincide with unity, all the other eigenvalues must be greater than unity when $\beta{=}\frac{1}{12}$. Therefore $\mathcal{S}_{min}(\beta){=}1$ for $\beta{\ge}\frac{1}{12}$. ∎

REMARK 5.1. *For n even, notice that $(0,0), (\pi,\pi), (0,\pi)$ and $(\pi, 0)$ can be represented on the mesh (see the definition of θ_N in (15)). Thus, the fastest and the slowest evolving eigenvalues with respect to the stabilization operator are $\Lambda(\pi,\pi,\beta){=}24\beta$ and $\Lambda(0,0,\beta){=}1$ with the maximum eigenvalue for $\beta{\ge}\frac{1}{24}$ being of multiplicity one given by $\Lambda(\pi,\pi,\beta){=}24\beta$. Also the smallest eigenvalue for $0{\le}\beta{\le}\frac{1}{12}$ is of multiplicity two and is given by $\Lambda(\pi,0,\beta){=}\Lambda(0,\pi,\beta){=}12\beta$.*

In view of the above remark it is convenient to assume that n is even and then take $\boldsymbol{\theta}^\star$ to be (π, π) and $\boldsymbol{\theta}^+{=}(0, \pi)$ or $(\pi, 0)$ in the following. Our main result is now stated in the following theorem.

THEOREM 5.5. *The condition number κ of the stabilized formulation (28), defined by*

$$\kappa(\beta) \equiv \frac{\Lambda_{max}(\beta)}{\Lambda_{min}(\beta)},$$

where $\Lambda_{max}(\beta){=}\max_{\boldsymbol{\theta}\in\Theta_N} \Lambda(\boldsymbol{\theta}, \beta)$ and $\Lambda_{min}(\beta){=}\min_{\boldsymbol{\theta}\in\Theta_N} \Lambda(\boldsymbol{\theta}, \beta)$, is minimized on the interval $[\frac{1}{24}, \frac{1}{12}]$.

Proof. We consider the intervals $I_1{=}(0, \frac{1}{24})$, $I_2{=}(\frac{1}{24}, \frac{1}{12})$, and $I_3{=}(\frac{1}{12}, \infty)$ separately. For $\beta{\in}I_1$ we have that $\Lambda_{max}(\beta){=}1$ and $\Lambda_{min}(\beta){=}12\beta$. Hence

$$\kappa = \frac{1}{12\beta} \quad \text{for } \beta \in I_1.$$

For $\beta{\in}I_2$ we have that $\Lambda_{max}(\beta){=}24\beta$ and $\Lambda_{min}(\beta){=}12\beta$. Thus

$$\kappa = \frac{24\beta}{12\beta} = 2 \quad \text{for } \beta \in I_2.$$

Finally, for $\beta{\in}I_3$, $\Lambda_{max}(\beta){=}24\beta$ and $\Lambda_{min}(\beta){=}1$ and so

$$\kappa = \frac{24\beta}{1} = 24\beta \quad \text{for } \beta \in I_3.$$

Consequently we have

$$\begin{aligned}
\frac{\mathrm{d}\kappa}{\mathrm{d}\beta} &= \frac{-1}{12\beta^2} < 0 \quad \text{for } \beta \in I_1, \\
\frac{\mathrm{d}\kappa}{\mathrm{d}\beta} &= 0 \quad \text{for } \beta \in I_2, \\
\frac{\mathrm{d}\kappa}{\mathrm{d}\beta} &= 24 > 0 \quad \text{for } \beta \in I_3.
\end{aligned}$$

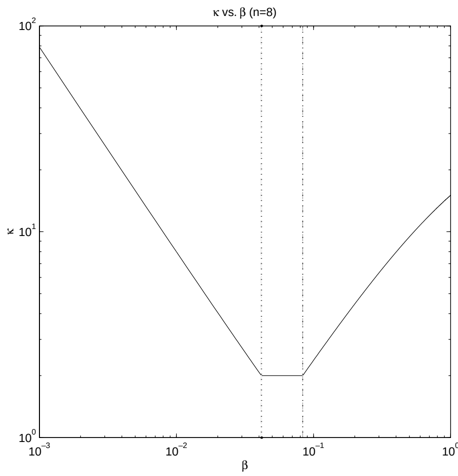

FIG. 6. *Condition of the stabilized pressure Schur complement corresponding to a Q_1-Q_1 approximation of a periodic Stokes problem on an* 8×8 *grid.*

Thus κ is minimized on I_2. $\square$

REMARK 5.2. *The optimal stabilization parameter β^* can be identified with the value which minimizes the condition number κ in Theorem* 5.5*; see Silvester* [10]. *The conclusion is that there is an interval of optimal stabilization parameter values.*

An illustration of how κ varies with β on a fixed grid is given in Figure 6 (the dotted lines indicate the parameter values $\beta=\frac{1}{24}$ and $\beta=\frac{1}{12}$). The plot is in exact agreement with the above analysis.

The final remark relates Theorem 5.5 to the case of more realistic (nonperiodic) boundary conditions.

REMARK 5.3. *Given general boundary conditions, an analysis based on eigenvalue bounds (see* [10] *and* [4, pp. 533–549]*) suggests a "default" choice of β; namely, $\beta_* = \Gamma^2/\Phi^2$ with*

$$\Gamma^2 = \max_{q_h\in Q_h}\max_{\mathbf{v}_h\in V_h}\frac{(q_h,\nabla\cdot\mathbf{v}_h)^2}{|\mathbf{v}_h|_1^2\|q_h\|_0^2} \quad \textit{and} \quad \Phi^2 = \max_{q_h\in Q_h}\frac{C_h(q_h,q_h)}{\|q_h\|_0^2}.$$

Here, Lemmas 4.6 *and* 5.2 *imply that $\Gamma^2 = 1$ and $\Phi^2 = 24$. Thus the suggested value β_* corresponds to an optimal value in the case of periodic boundary conditions.*

6. Extensions. It is obvious that Fourier analysis may be used to study stabilization of any equal-order approximation of a periodic Stokes flow problem. For triangular elements, however, the identification of the particular value β^* minimizing κ as defined in Theorem 5.5 is not straightforward, unlike the square element case.

One specific result that we have established in the case of stabilized P_1-P_1 approximation on a uniform mesh of bisected squares is that $\beta=\frac{11}{288}$ minimizes the quantity $\Lambda_{max}-\Lambda_{min}$. That is, at $\beta=\frac{11}{288}$ the *width* of the spectrum corresponding to (29) is minimized. An illustration of how the P_1-P_1 condition number varies in practice is given in Figure 7 (here the dotted line indicates the parameter value $\beta=\frac{11}{288}$). Notice that, in contrast to the Q_1-Q_1 case, the "optimal" value appears to be unique.

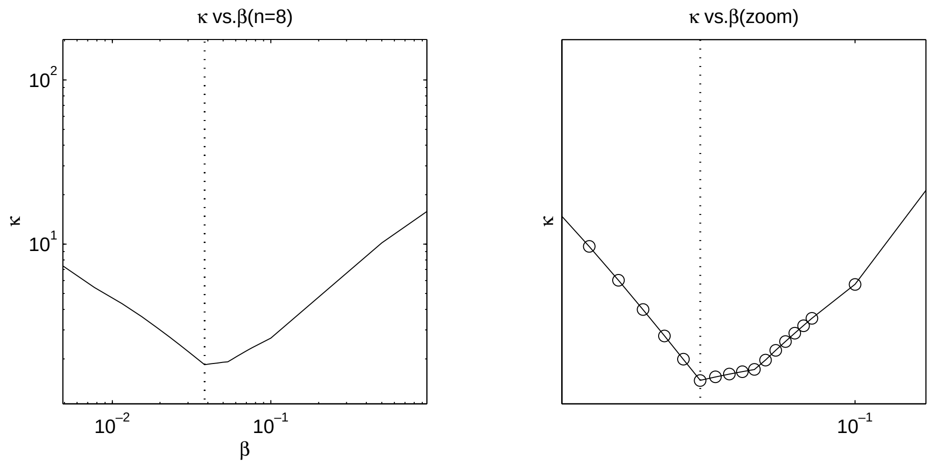

FIG. 7. *Condition of the stabilized pressure Schur complement corresponding to a* P_1*-*P_1 *approximation of a periodic problem on a bisected* $8{\times}8$ *grid.*

REFERENCES

[1] F. BREZZI AND J. PITKÄRANTA, *On the stabilization of finite element approximations of the Stokes problem*, in Efficient Solutions of Elliptic Systems, W. Hackbusch, ed., Vieweg, Braunschweig, 1984, pp. 11–19.

[2] F. BREZZI AND J. DOUGLAS, *Stabilized mixed methods for the Stokes problem*, Numer. Math., 53 (1988), pp. 225–235.

[3] V. GIRAULT AND P. A. RAVIART, *Finite Element Methods for Navier-Stokes Equations–Theory and Algorithms*, Springer-Verlag, Berlin, 1986.

[4] P. M. GRESHO AND R. SANI, *Incompressible Flow and the Finite Element Method*, Wiley, Chichester, UK, 1998.

[5] R. A. HORN AND C. R. JOHNSON, *Matrix Analysis*, Cambridge University Press, Cambridge, UK, 1985.

[6] T. J. R. HUGHES, L. FRANCA, AND M. BALESTRA, *A new finite element formulation for CFD:* V. *Circumventing the Babuska-Brezzi condition: A stable Petrov-Galerkin formulation of the Stokes problem accommodating equal-order interpolations*, Comput. Methods Appl. Mech. Engrg., 59 (1986), pp. 85–99.

[7] S. IDELSOHN, M. STORTI, AND N. NIGRO, *Stability analysis of mixed finite element formulations with special mention of equal order interpolations*, Internat. J. Numer. Methods Fluids, 20 (1995), pp. 1003–1022.

[8] S. NORBURN AND D. SILVESTER, *Stabilized vs. stable mixed methods for incompressible flow*, Comput. Methods Appl. Mech. Engrg., 166 (1998), pp. 131–141.

[9] G. SEGAL, K. VUIK, AND K. KASSELS, *On the implementation of symmetric and antisymmetric periodic boundary conditions for incompressible flow*, Internat. J. Numer. Methods Fluids, 18 (1994), pp. 1153–1165.

[10] D. SILVESTER, *Optimal low order finite element methods for incompressible flow*, Comput. Methods Appl. Mech. Engrg., 111 (1994), pp. 357–368.

[11] D. SILVESTER AND A. WATHEN, *Fast iterative solution of stabilized Stokes systems part* II: *Using general block preconditioners*, SIAM J. Numer. Anal., 31 (1994), pp. 1352–1367.

[12] G. STOYAN, *Towards discrete Velte decompositions and narrow bounds for inf-sup constants*, Comput. Math. Appl., 38 (1999), pp. 243–261.

[13] R. TEMAM, *Navier-Stokes Equations and Nonlinear Functional Analysis*, CBMS-NSF Reg. Conf. Ser. in Appl. Math., 66 SIAM, Philadelphia, 1995.